

Real-Time Quality Assessment of Long-Term ECG Signals Recorded by Wearables in Free-Living Conditions

Lukas Smital ^{ID}, Clifton R. Haider ^{ID}, Member, IEEE, Martin Vitek ^{ID}, Pavel Leinveber ^{ID}, Pavel Jurak, Andrea Nemcova ^{ID}, Radovan Smisek ^{ID}, Lucie Marsanova ^{ID}, Ivo Provaznik ^{ID}, Member, IEEE, Christopher L. Felton, Barry K. Gilbert, and David R. Holmes III

Abstract—Objective: Nowadays, methods for ECG quality assessment are mostly designed to binary distinguish between good/bad quality of the whole signal. Such classification is not suitable to long-term data collected by wearable devices. In this paper, a novel approach to estimate long-term ECG signal quality is proposed. **Methods:** The real-time quality estimation is performed in a local time window by calculation of continuous signal-to-noise ratio (SNR) curve. The layout of the data quality segments is determined by analysis of SNR waveform. It is distinguished between three levels of ECG signal quality: signal suitable for full wave ECG analysis, signal suitable only for QRS detection, and signal unsuitable for further processing. **Results:** The SNR limits for reliable QRS detection and full ECG waveform analysis are 5 and 18 dB respectively. The method was developed and tested using synthetic data and validated on real data from wearable device. **Conclusion:** The proposed solution is a robust, accurate and computationally efficient algorithm for annotation of ECG signal quality that will facilitate the subsequent tailored analysis of ECG signals recorded in free-living conditions. **Significance:** The field of long-term ECG signals self-monitoring by wearable devices is swiftly developing. The analysis of massive amount of collected data is time consuming. It is advantageous to characterize data quality in advance and thereby limit consequent analysis to useable signals.

Index Terms—ECG delineation, ECG signal, QRS detection, signal quality, signal segmentation, SNR estimation.

Manuscript received September 3, 2019; revised December 23, 2019; accepted January 14, 2020. Date of publication January 27, 2020; date of current version September 18, 2020. This work was supported in part by the United States Office of Naval Research Global under Grant N62909-19-1-2006 and in part by the National Program of Sustainability II (MEYS CR) Project LQ1605. (*Corresponding author: Lukas Smital.*)

L. Smital is with the Department of Biomedical Engineering, Brno University of Technology, Brno 61600, Czech Republic (e-mail: smital@feec.vutbr.cz).

C. R. Haider, C. L. Felton, B. K. Gilbert, and D. R. Holmes III are with the Department of Physiology and Biomedical Engineering.

M. Vitek, A. Nemcova, R. Smisek, L. Marsanova, and I. Provaznik are with the Department of Biomedical Engineering, Brno University of Technology.

P. Leinveber is with the International Clinical Research Center, St. Anne's University Hospital.

P. Jurak is with the Institute of Scientific Instruments of the Czech Academy of Sciences.

Digital Object Identifier 10.1109/TBME.2020.2969719

I. INTRODUCTION

ACCORDING to the World Health Organization (report from May 2017), cardiovascular diseases (CVD) are responsible for approximately 30% of all deaths worldwide [1]. In addition, nearly 80% of all cardiovascular-related deaths occur in low- and middle-income countries [2]–[4]. The most common diagnostic method used to detect heart disease is measuring the heart's electrical activity by electrocardiography (ECG). Nowadays, the telemedicine area and the field of long-term self-monitoring not only of patients but also of athletes are swiftly developing. For this purpose, wearable devices are often used. Their advantage is small size, sufficient battery life and relative affordability. On the other hand, the record quality generally fluctuates because sensing is done in free-living conditions in comparison with ambulatory resting ECG. Long-term ECG monitoring data often contain a variety of artifacts (e.g., powerline interference, drift, impulse noise, and muscle noise) that complicate subsequent analysis [5]. The change of noise intensity over time and overall non-stationarity of the signal also complicate the processing of the long-term signals.

The issue of ECG quality evaluation has recently become a hot topic [6]–[10]. There are many reasons for signal quality evaluation from suppressing false alarms [7], [11] through recognizing poor skin-electrode contact [12], selecting segments for extracting clinically relevant features [13], [14], or further processing the signal guaranteeing its interpretation quality [15]. Many investigators have proposed algorithms based on the extraction of statistical or morphological features from the signal. For example, Orphanidou *et al.* [16] proposed signal quality indices (SQI) based on the success of QRS complexes detection, the physiology of the measured heart rate, and variation in the length of RR intervals. Meanwhile, Wang [17] compared the similarity of successive QRS complexes, as significant differences between QRS complexes may indicate the presence of a large amount of noise. Li *et al.* [18] used a heart rate signal derived from the ECG signal and measurements of arterial blood pressure to determine the SQI, while Bartolo *et al.* [19] estimated the signal quality based on the deviations in the lengths of RR intervals and noise estimation after matched filtration of the ECG with the QRS template. Allen and Murray [20] calculated the mean level of six different frequency bands of the ECG signal and counted

out-of-range events in 10 seconds window. This information was subsequently used for bad signal quality recognition. The main disadvantages of these methods are their dependency on reliability and accuracy of QRS complex detection and the fact they do not estimate the true level of noise in the signal but only parameters that are indirectly related with noise.

The proposed algorithm can automatically determine the quality of the ECG signal prior to analysis which is especially important in the case of long-term recording by Holter monitors or other experimental devices [21], [22]. The algorithm estimates the continuous signal-to-noise ratio (SNR) of the data and consequently determines segments in which the quality of the ECG signal is not significantly changing (SNR is within the defined range). Based on signal quality, as determined by this algorithm, segments of the ECG signal may be subjected to additional analysis, using software specific to the signal quality. Importantly, the proposed approach permits analysis of the massive amount of data collected by wearable devices more effectively. First, a noise-free signal is estimated by Wavelet Wiener Filter (WWF) [23]. The SNR can be calculated in one of two ways, i.e., in either the time or time-frequency domain. In both cases, the calculation is performed in a sliding window of specified length, allowing real-time processing. In the next step, the ECG signal is segmented according to the measured continuous SNR curve, and subsequently a different processing methods can be applied to individual segments. In this way, complicated analysis of poor-quality data can be avoided, and more importantly, algorithms that are tuned according to the signal quality can be used. Advantages of proposed method over prior methods are its independency on the QRS complex detection and the fact that directly estimates the ECG signal SNR value continuously over the time.

II. MATERIALS AND METHODS

In this paper, a novel and robust algorithm to assess ECG signal quality based on continuous SNR estimation and consequent signal segmentation is proposed. By measuring the quality of the ECG signal continuously, it is determined which segments of the signal are suitable for further processing and which are not. However, before the signal can be divided into different segments according to quality, the quality classes must be defined. In cooperation with Holter ECG experts, three logical quality classes were selected for this analysis: (Q1) segments that exhibit such a low noise level that allow any common type of analysis including full ECG wave analysis; (Q2) segments that contain such a level of noise that allow reliable QRS complex detection and thus basic rhythm analysis; and (Q3) segments that contain such levels of noise that further processing is precluded because even QRS complex detection and thus basic rhythm analysis is not reliable.

The proposed algorithm principle is presented in Fig. 1. At the input of the block SNR_{est} (SNR estimation), there is generally ECG signal with a changing quality. In this block, SNR is continuously estimated in two steps. Firstly, the noise-free signal and noise are estimated by the WWF method. Secondly, the SNR is calculated from these signals in the sliding window. The result

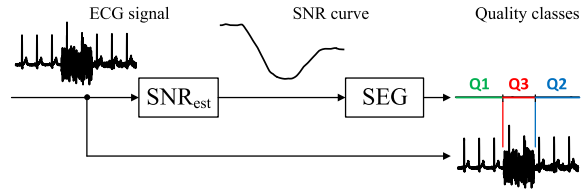


Fig. 1. Proposed ECG signal quality assessment process.

is the continuous SNR curve tracking the signal quality (see SNR_{est} output in Fig. 1). The block SEG (segmentation) uses the continuous SNR curve as the input. The segmentation itself uses decision rules based on SNR thresholds and duration limits to determine boundaries between segments of different qualities (see the output of the block SEG in Fig. 1). The final result of the whole ECG quality estimation process is the annotations marking segments boundaries. The original input ECG signal remains at the output untouched. The whole processing pipeline including the used data is described in detail below.

A. Datasets

Two different ECG datasets to test the proposed algorithms were used. The first is artificially created ECG dataset for which the used defined parameters such as SNR setting are known. The second is a real dataset acquired by a specially designed wearable ECG device [24]. All human studies were approved by Mayo Clinic's Institutional Review Board, under Mayo IRB Protocol #10-006608 00 on Dec. 7, 2010. Informed written consent was obtained from all subjects prior to the studies.

1) Artificial Dataset: The artificial dataset was created using the combinations of two different artificial noise-free ECG signal types and three different noise types. A database of 250 different signals with duration of 30 minutes and sampling frequency (f_s) 512 Hz was generated including each of the six possible combinations of noise-free signal and noise type. The detail settings are described below.

Periodic noise-free ECG signal was created by careful filtering and consequently repeating one cycle of real ECG signal from the "Common Standards for Quantitative Electrocardiography" database [25], [26] with minimal noise.

Realistic noise-free ECG signal was generated using tool (*ecgsyn.m*) from PhysioNet [27] and described in detail by McSharry *et al.* [28]. The tool parameters values were generated randomly within a given range: mean heart rate (50–180 beats per minute), standard deviation of heart rate (1–10 beats per minute) and low/high frequency ratio (0.5–8.9).

EcgSyn noise was also generated using the tool [28]. This noise has uniform distributed random values of samples.

Real muscle artifact is a record of muscle noise from MIT-BIH Noise Stress Test Database [29] on PhysioNet [27].

Model muscle noise was generated by filtering white Gaussian noise described by Farina *et al.* [30]–[32]. Model of the surface EMG power spectra is created using a shaping filter

$$H[f] = \frac{f_h^4 f^2}{(f^2 + f_t^2)(f^2 + f_h^2)^2}, \quad (1)$$

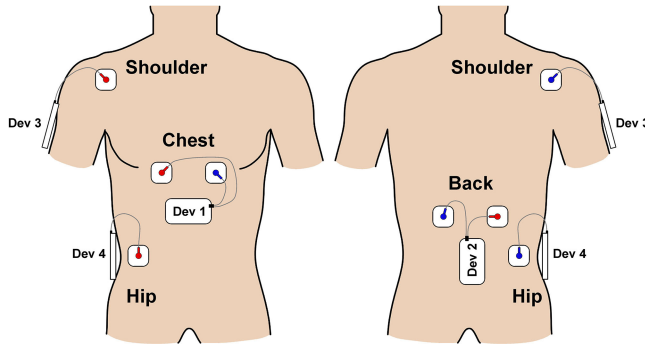


Fig. 2. Placement of devices and leads on the subject body.

where the parameters f_h and f_l change the shape of the spectral function. In our study, we used parameters $f_h = 46$ Hz and $f_l = 346$ Hz.

For purposes of further testing, the required SNR time course can be set by changing the amplitude of the noise, as described by Smital *et al.* [23].

2) Real Dataset: The real ECG dataset was obtained by complex 50 minutes measurement of three subjects during performing predefined physical activities. The dataset contains a total of 10 types of activities (supine, sitting, standing, squats, slow deep breathing, quick deep breathing, breath hold, tilt table test, Valsalva maneuver, Müller's maneuver). Simultaneously, ECG signals from four different spots on the subject body (chest, back, shoulder and hip) by four devices of the same type were measured. Placement of electrodes can be seen in the Fig. 2. Each device includes a one-lead configuration for high resolution ECG data collection. The device incorporated a custom low power ($100 \mu\text{W}$ at a 2.8 V supply voltage) ECG circuit with 100 dB common mode rejection [24]. In addition, to capture posture and physical activity, each device also contained 2 g (VTI Technologies, CMA3000-A01) and 16 g tri-axial accelerometers (Analog Devices, ADXL326BCPZ) [33]–[35]. The device data acquisition rates for both ECG and motion are programmable, and were set to 400 samples per second for the ECG monitor and 10 samples per second per individual x-, y-, and z-axis, respectively. This device configuration allows continuous recording for 14 days on a single 750 mAh battery (Bi-power, BL-7PN-S2). The obtained ECG signals differ in quality among the individual leads (measured on four different body spots) and also vary in time (performing different activities). Raw synchronization among different devices is performed by taping on all devices at the same time at the beginning of the measurement. Taps are visible in accelerometer data. Fine synchronization is performed by QRS detection in the ECG signals from all 4 devices and consequent alignment of these signals according to RR intervals. In the same time, standard 12-lead ECG was measured as a reference.

B. Continuous SNR Estimation Algorithm

The SNR was chosen as a quality metric of the ECG signal. The main reason is that the SNR is directly related with the level of noise present in the ECG signal and the estimate of the SNR

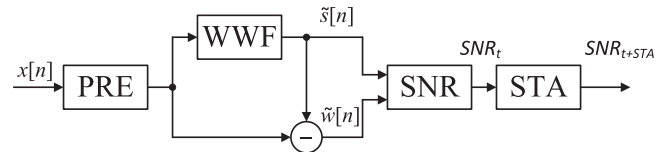


Fig. 3. Block diagram of SNR estimation algorithm using the sliding window approach.

values can be calculated in real-time in a sliding window directly on the wearable device. The result of the SNR estimation is thus a SNR curve tracking the ECG signal quality continuously over the time. To estimate the ECG signal quality correctly, it must be defined what it is considered as noise levels that would complicate diagnosis. Such a noise has components that cannot be simply removed from the ECG signal by common preprocessing methods without corrupting the noise-free component. In particular, only broadband interferences exhibiting spectra overlapping with the spectrum of the ECG signal and thereby rule out linear filtering are considered. The most common case of this type of interference in ECG records is EMG. Conversely, narrowband interference such as drift or powerline interference can be easily eliminated and do not affect subsequent ECG analysis. For the purpose of assessing the ECG signal quality with regard to subsequent analysis, it is therefore correct to remove drift and powerline interference from the ECG signal in preprocessing, and to take into account only broadband interference in the calculation of the SNR. For example: An ECG signal with significant drift (easily removable) have a reduced SNR value when considering this type of interference, and could be wrongly classified as Q2 or even Q3, although it has a high diagnostic value and it is suitable for full wave analysis (Q1 category) after preprocessing. To estimate the SNR curve, two approaches were tested: ii) a time domain approach and, ii) a time-frequency domain approach.

1) Time Domain Approach of Continuous SNR Estimation: The time domain approach is illustrated in the block diagram in Fig. 3. The preprocessing part PRE involves cascaded high pass and notch digital filters. The high pass filter is FIR filter of 1000th order with cutoff frequency 0.67 Hz which eliminates baseline wander (caused e.g., by movement or respiration) [36]. The notch filter is also FIR filter of 1000th order with cutoff frequencies 49.2 and 50.8 Hz which eliminates powerline interference.

After the preprocessing it is assumed that the examined digital signal $x[n]$ is an additive mixture of noise-free signal $s[n]$ and broadband noise $w[n]$, according to the equation $x[n] = s[n] + w[n]$, where n represents the digital time sequence. Precise estimation of the noise-free signal is essential for accurate SNR calculating. The approach uses the Wavelet Wiener Filtering method (WWF), a two-stage algorithm operating in the wavelet domain [37], [38]. In the first stage, thresholding of the wavelet coefficients of preprocessed input signal $x[n]$ is used to estimate the noise-free signal coefficients $u_m[n]$ (settings: wavelet db4, decomposition level 4, nonnegative garrote thresholding). The details are described in our previous study Smital *et al.* [23, Ch. II. B and II. C]. In the second stage, the Wiener correction

factor $g_m[n]$ is computed according to equation (2), where $\sigma_m^2[n]$ is the variance of the noise coefficients in the m th frequency band. Variance is estimated using the median according to (3). Coefficients $y_m[n]$ obtained by wavelet transform (settings: wavelet *sym4*, decomposition level 4) of preprocessed input signal $x[n]$ are adjusted according to equation (4), where $\tilde{y}_m[n]$ is the estimation of the denoised wavelet coefficients. By transforming the coefficients $\tilde{y}_m[n]$ back to the time domain using inverse wavelet transform, the denoised signal estimation $\tilde{s}[n]$ is obtained.

$$g_m[n] = \frac{u_m^2[n]}{u_m^2[n] + \sigma_m^2[n]} \quad (2)$$

$$\sigma_m^2[n] = \left(\frac{\text{median}(|y_m[n]|)}{0.6745} \right)^2 \quad (3)$$

$$\tilde{y}_m[n] = y_m[n] \cdot g_m[n] \quad (4)$$

The estimated noise $\tilde{w}[n]$ is computed by subtracting the noise-free signal estimate $\tilde{s}[n]$ from the preprocessed input signal $x[n]$.

The SNR block computes the local energy of the estimation of noise-free signal $\tilde{s}[n]$ and noise $\tilde{w}[n]$ bounded by window (W) with duration of 2 seconds. The longer the window, the slower is the response of the output SNR curve to the change of real SNR in the signal. The shorter the window, the greater the oscillation of the output SNR curve. Two second window was selected as the compromise between dynamicity and amplitude of the oscillation of the output SNR curve. Such a length ensures that the window always contains all the components of the ECG cycle (at least one whole ECG cycle), even at a low heart rate (30 bpm). The larger window would cause a loss of dynamics of the resulting SNR curve. The SNR estimation ($SNR_t[n]$) is computed in decibels according to

$$SNR_t[n] = 10 \cdot \log_{10} \left(\frac{\sum_{j=n-W/2}^{n+W/2} (\tilde{s}[j])^2}{\sum_{j=n-W/2}^{n+W/2} (\tilde{w}[j])^2} \right) \text{dB.} \quad (5)$$

Due to the fixed size of window W , the estimate of SNR is oscillating with the changing number of QRS complexes within the window. This problem solves the last block of short-time averaging STA where samples of SNR_t are averaged in a sliding window with duration of 2 seconds. The final product of the whole approach is the averaged curve SNR_{t+STA} .

2) Time-Frequency Domain Approach of Continuous SNR Estimation: The second approach for estimating SNR is using a spectrogram (SG) which represents the amplitude spectrum over time obtained by the STFT (Short Time Fourier Transform). The principle is shown in Fig. 4.

The first three steps (Preprocessing, Wavelet wiener filtering and signal subtracting) are the same as in the case of the time domain approach. In the next step, signals $\tilde{s}[n]$ and $\tilde{w}[n]$ enter the STFT blocks where are calculated their spectrograms SG_s (spectrogram of the noise-free signal) and SG_w (spectrogram of the noise estimations). The SNR block computes the local energy in the spectrograms using sliding window W with duration of 2 seconds. The SNR estimation (SNR_{tf}) is computed in

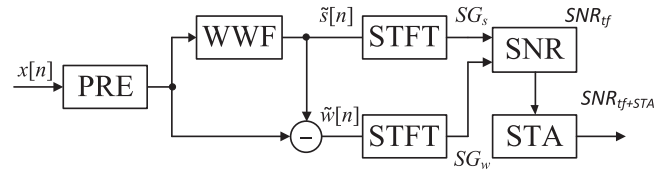


Fig. 4. Block diagram of SNR estimation algorithm by STFT frequency approach.

decibels according to

$$SNR_{tf}[n]$$

$$= 10 \cdot \log_{10} \left(\frac{\sum_{i=0}^{f_s/2} \sum_{j=n-W/2}^{n+W/2} (SG_s[i, j])^2}{\sum_{i=0}^{f_s/2} \sum_{j=n-W/2}^{n+W/2} (SG_w[i, j])^2} \right) \text{dB.} \quad (6)$$

The whole frequency range was used ($0 - f_s/2$), but the method can be easily modified to work with a limited frequency range depending on the purpose of the application/signal.

From the same reasons as in the previous method, the block STA is used (the setting is identical). The result of this approach is averaged curve SNR_{tf+STA} .

3) SNR Estimation Methods Demonstration: To demonstrate the principle and functionality of the designed SNR estimators, signal with artificially set SNR course was used and the estimators tried to estimate it. Both artificial ECG signal types (periodic and realistic noise-free ECG signal) and model muscle noise described above were used. This noise was generated with a gradually changing level. The set three levels of the noise represent defined ECG signal quality classes: -10 dB for large interference (representing the Q3 quality class where even QRS complexes are hidden within the noise), 10 dB for moderate interference (representing the Q2 quality class where only QRS complexes can be reliably detected), and 30 dB for low interference (representing the Q1 quality class allowing full-wave analysis of the ECG signal).

The results of methods are shown in the Fig. 5. In the upper part of the figure, there is an artificial mixture of the noise with changing level and the ECG signal (black curve). Red curve represents the estimate of the noise-free signal $\tilde{s}[n]$ (output of the WWF block). True preset noise level (black) as well as estimated SNR courses by both methods are shown in the lower part of the figure. The result of the time domain approach is presented by blue solid line and the time-frequency domain approach by red solid line. It can be concluded that both estimators yield approximately equal results, and both are similar to the preset noise level. Estimates of the SNR exhibit the largest error from the known SNR at the artificial transitions between SNR levels.

In the right part of the Fig. 5 is demonstrated the need of the STA in the last step of the process. Input of the STA are SNR courses which are oscillating. These oscillations in the SNR estimation (black arrows) are related to the fixed window size W (2 s) and a variable number of QRS complexes within the sliding window (gray squares). By using STA, smoothed SNR courses are obtained.

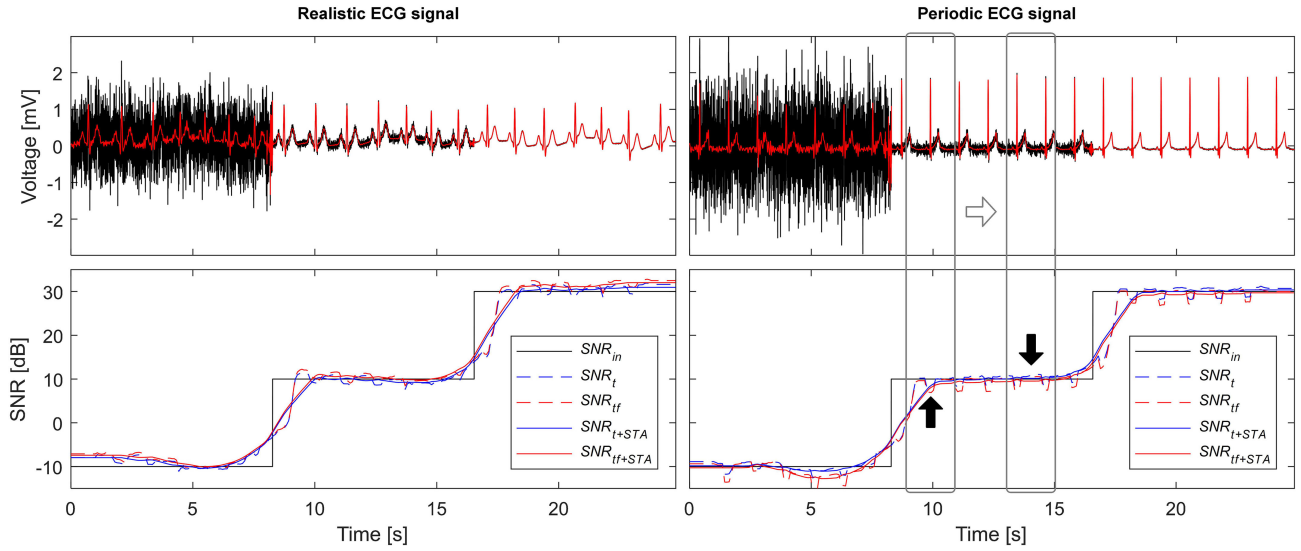


Fig. 5. Top: Artificial ECG signals with changing noise level (black) and estimates of noise-free signal by WWF (red). Bottom: Comparison of estimated SNR courses in the time domain (blue) and the time-frequency domain (red), before (dashed line) and after (solid line) the STA. The black curve is the preset level of SNR in the input signal. The gray squares in the right part of the figure represent sliding window while black arrows mark oscillations.

C. ECG Signal Segmentation

ECG signal segmentation itself is the process of identifying the positions within the ECG where the signal quality class changes. At the same time, segments where the quality remains unchanged are identified. The final product of the whole process is then ECG signal with quality annotation. To realize the segmentation process, SNR thresholds setting must be firstly defined. It lies in finding specific SNR values discriminating the quality classes and set up rules for segmentation itself.

1) SNR Threshold Setting Criteria: Since there were defined three ECG signal quality classes Q1, Q2 and Q3, it is searched for two SNR threshold level values separating the class Q1 from class Q2 and class Q2 from class Q3. For segments of Q1 quality class, which are suitable for full ECG wave analysis, it is possible to reliably detect the QRS complex and five other significant points in the ECG curve (P onset, P offset, QRS onset, QRS offset, T offset). It must be possible to reliably detect the QRS complexes to satisfy the criteria for quality class Q2. In the segments of Q3 quality class, reliability of QRS complex detection is not guaranteed.

For distinguishing between Q2 and Q3 quality classes, it must be found the threshold SNR value where QRS detection changes from reliable to unreliable. As a criterion of reliable QRS detection it is considered where both sensitivity (Se) and positive predictive (P^+) values are greater than 99.5% [39]. These statistical parameters are defined respectively as

$$Se = \frac{TP}{TP + FN}, \quad P^+ = \frac{TP}{TP + FP}, \quad (7)$$

where TP represents true positive values (correctly detected points), FN represents false negative values (undetected points), and FP represents false positive values (incorrectly detected points). The detected position is identified as TP when the deviation from a reference position is less than 50 ms. This

TABLE I
CRITERIA 2sCSE FOR STANDARD DEVIATION OF DETECTION ERROR

P_{on}	P_{off}	QRS_{on}	QRS_{off}	T_{off}
10.2 ms	12.7 ms	6.5 ms	11.6 ms	30.6 ms

value has been taken over from a paper by Zidelman *et al.* as a tolerance window normally used for QRS detection [40].

For distinguishing between Q1 and Q2 quality class, it must be found threshold SNR value where standard ECG delineation (detection of five ECG significant points) changes from reliable to unreliable. As a criterion of reliable ECG delineation, it is considered the standard deviation of differences between the reference and detected positions, which must be for all significant points less than the limits specified in Table I. These limits were published by Willems *et al.* in [41].

2) SNR Segmentation Rules: The input of the segmentation algorithm is the continuous SNR curve. The ECG segmentation algorithm (the process of labelling a dataset with Q1, Q2, and Q3) consists of two steps: basic segmentation and correction. The basic segmentation naively labels temporal segments solely on the basis of two SNR thresholds distinguishing between quality classes. The crossing of one of the thresholds marks the end of one segment and the beginning of another. However, the SNR level can change rapidly (particularly during motion), which can lead to excessive quality fragmentation. For example, in the case where the SNR value oscillates around one of the thresholds. Too many too short segments may complicate subsequent analysis. Accordingly, correction rules may be applied to reasonably connect the adjacent segments. It is advantageous to eliminate those segments which are too short to be meaningfully analyzed or if the SNR crossed the threshold only a little by joining those segments to adjacent segments. The segment joins are accomplished by eliminating border labels. Two separate

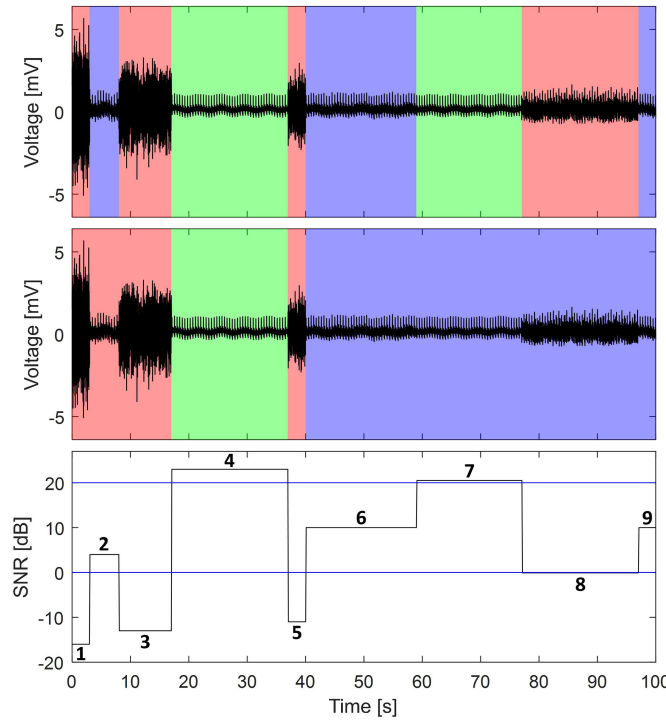


Fig. 6. Top: The result of artificial ECG signal segmentation using only SNR thresholds. Green color highlights segments of Q1 quality, blue color highlights segments of Q2 quality and red color highlights segments of Q3 quality. Middle: The result of artificial ECG signal segmentation using both SNR thresholds and correction rules. Bottom: Setting of artificial ECG signal SNR levels. SNR thresholds are marked blue.

sets of correction rules were defined; one for a higher SNR signal falling within a lower SNR signal, and a second for a lower SNR signal falling within a higher SNR signal. In the first case, when a higher SNR signal is shorter than 15 seconds, or its average SNR value is within 1 dB of the label threshold, the segment is ignored (i.e., labeled as lower SNR similar to adjacent segments). In contrast, for a lower SNR segment shorter than 3 seconds, or where the average SNR value is within 1 dB of the label threshold, the lower SNR signal is treated as if it were a higher SNR signal (i.e., labeled as higher SNR similar to adjacent segments).

The values of correction rules (15 sec, 3 sec and 1 dB) were designed heuristically with respect to the need of the real dataset analysis. These rules can be adjusted for different use cases or can be even omitted.

3) Segmentation Method Demonstration: To demonstrate the functionality of proposed segmentation algorithm, it was created an artificial ECG signal using realistic ECG generator and model muscle noise with 9 various levels, **Fig. 6**. The segmentation algorithm was designed to work in a real-time mode with 15 seconds buffer. The results of segmentation demonstration are plotted in **Fig. 6**. Top part of **Fig. 6** highlights the result of basic segmentation using only SNR thresholds, which were set as 0 and 20 dB. This setting is only a heuristic rough estimate based on noise levels in **Fig. 5**. The setting of exact SNR thresholds values is the part of the results. It can be observed 9 segments in

total as an output of the proposed method. Middle part of **Fig. 6** highlights the result of segmentation using both SNR thresholds and correction rules. The correction rules joined segment No. 2 with segments No. 1 and No. 3 because the segment was too short. Similarly, segments No. 7 and No. 8 were joined with segments No. 6 and No. 9 because they were determined to have barely crossed the SNR thresholds, how can be seen from bottom part of **Fig. 6**. The result are 4 segments suitable for consequent tailored analysis.

III. RESULTS

The methodology for continuous SNR estimation and ECG signal segmentation has been proposed. In this chapter, the reliability of the SNR estimate is objectively evaluated, threshold values for segmentation are determined and the segmentation itself is demonstrated. For these purposes, the artificial dataset is used. Finally, the complete segmentation pipeline is applied on real data.

A. Artificial Dataset

1) Testing of SNR Estimation Accuracy: In this part, the SNR estimation accuracy of both designed methods is tested: 1) Time domain approach and 2) Time-frequency domain approach. The range of SNR values in which the estimation reliable needs to be determined. The common range of SNR values in ECG signals is between -5 and 55 dB [23]. The tested scale of SNR values was selected with a reserve from -40 to 80 dB with a step of 1 dB. The testing was carried out on an artificial dataset created by combining realistic noise-free ECG signals with model muscle noise. Each of 250 signals was contaminated by 121 different noise levels. The testing database consists of 30 250 signals of 30 minute duration.

The results of testing are plotted in **Fig. 7**. The black curves represent estimated SNR values of all 250 signals which can deviate from ideal estimate represented by green line. It is obvious that the estimate is accurate within the range from -20 to 30 dB represented by blue dash dot lines. As a quality criterion of estimation accuracy, it was chosen to use mean and standard deviation between preset and estimated values. Within the range from -20 to 30 dB, the calculated mean and standard deviation using time domain approach are 0.21 and 0.72 dB respectively. The results for time-frequency domain are 1.04 and 0.93 dB. These values may be selected to be even lower because of the possibility to extract the systematic mistake represented by red curve which is obtained as a mean of all black curves. After the extraction, the calculated mean and standard deviation using time domain approach are 0 and 0.43 dB respectively and for time-frequency domain 0 and 0.76 dB. It is obvious that the time domain approach is superior and thus it is used further. However, the errors of both methods are small enough to be corrected by the 1 dB correction rule at the segmentation stage which was described above. Even though that SNR of ECG signals can be higher than 30 dB, there is a need to accurately estimate SNR only around segmentation thresholds. Apart from these thresholds the estimation can be quite rough. The thresholds values can be found below.

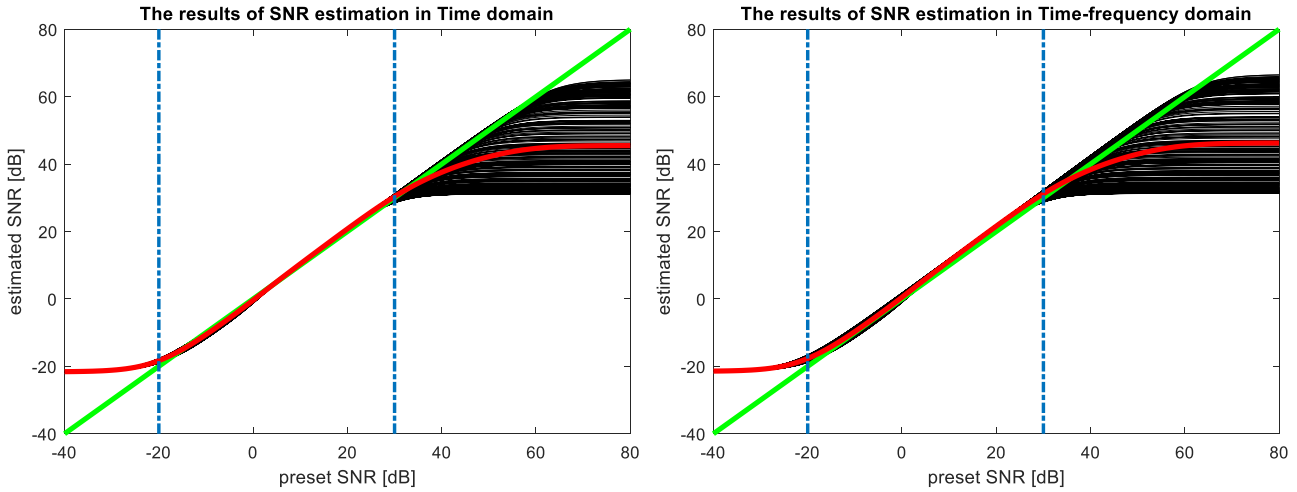


Fig. 7. Results of SNR estimation using Time domain approach (left) and Time-frequency domain approach (right). The black curves represent estimated SNR values on artificial dataset. The green line represents best possible estimate. The red curve represents the mean of black curves. The blue dash dot lines mark the range of accurate SNR estimation.

TABLE II
RESULTS OF TESTING QRS DETECTION AND ECG DELINEATION ALGORITHM ON SIX ARTIFICIAL DATASETS

Signal	Noise	Q2/Q3 threshold [dB]	Q1/Q2 threshold [dB]
Realistic noise-free ECG	Model muscle noise	3.4	17.8
	Ecgsyn noise	-0.4	14.6
	Real muscle artifact	4.4	14.2
Periodic noise-free ECG	Model muscle noise	0.6	15.8
	Ecgsyn noise	-3.8	14.6
	Real muscle artifact	2.4	11.8

2) SNR Threshold Setting: In this part, there is searched for two SNR thresholds setting which permits to distinguish between defined three quality classes. For this purpose, previously published methods for QRS complex detection [42] and ECG delineation [43], [44] were used. The SNR value, where QRS detector Se and P^+ crosses 99.5% distinguishes between quality classes Q2 and Q3. The SNR value, where ECG delineation algorithm crosses the acceptable standard deviation for all five ECG significant points (see. Table I) distinguishes between quality classes Q1 and Q2. For testing purposes, six artificial datasets were created by combining two types of noise-free signal with three types of noise. Each dataset contains 150250 signals with 30 minutes duration which were obtained by gradually increasing the SNR from -40 to 80 dB with 0.2 dB step on 250 signals.

The results of testing QRS detection and ECG delineation algorithm on all artificial datasets are provided in Table II. The estimated SNR threshold values differ between datasets. The global SNR thresholds were chosen to represent the most difficult combinations of signal and noise in order to minimize the risk of classifying the signal segment quality higher than actuality. The lower threshold was set as 5 dB (by rounding up 4.4) and the higher threshold was set as 18 dB (by rounding up 17.8). The rounding up was selected with respect to SNR estimation error.

The visualization of results for QRS detection (realistic noise-free ECG signal with Real muscle artifact) and ECG delineation (Realistic noise-free ECG signal with Model muscle noise) based on preset SNR is shown in Fig. 8. The QRS complex detection Se achieves the limit of 99.5% at 2.8 dB, while P^+ achieves the same limit at 4.4 dB. Thus, the threshold value was set based on P^+ . The last ECG delineation limit of 6.5 ms was crossed by QRS onset at 17.8 dB and thus the threshold was based on it.

3) Testing of Segmentation Method Accuracy: In this part, the accuracy of the whole segmentation pipeline is tested. As the accuracy criterion were chosen two different standard approaches: i) Se and P^+ of segments borders detection including mean and standard deviation calculation; ii) Coincidence matrix of segments quality classification. The testing used an artificial dataset created by combining realistic noise-free ECG signals with model muscle noise. The artificial dataset consists of 250 signals with duration of 30 minutes. Each of these signals was generated with random parameters settings: number of segments, segments duration and SNR levels. The reference quality segments were obtained by applying the proposed segmentation algorithm on known (generated) SNR curves of all signals and verified by Holter ECG experts.

The results of testing are shown in Table III and Table IV. In Table III, the effects of ECG quality segments borders detection is demonstrated to be pronounced. Specifically, the Se in both algorithm versions (with/without correction rules) is near 90%. On the other hand, the P^+ with correction rules is near 90% while without correction rules the P^+ is under 40%. The mean and standard deviation for both algorithm versions are under 100 ms and 1 s respectively. The mean reference number of segments per signal when not considering correction rules is 19.3. In the case of considering correction rules, this number reduces to 15.6. The mean detected number of segments by algorithm with correction rules is 16.1 per signal which is close to its reference value. In the case of algorithm without correction rules, the mean detected number of segments per signal is 60.6

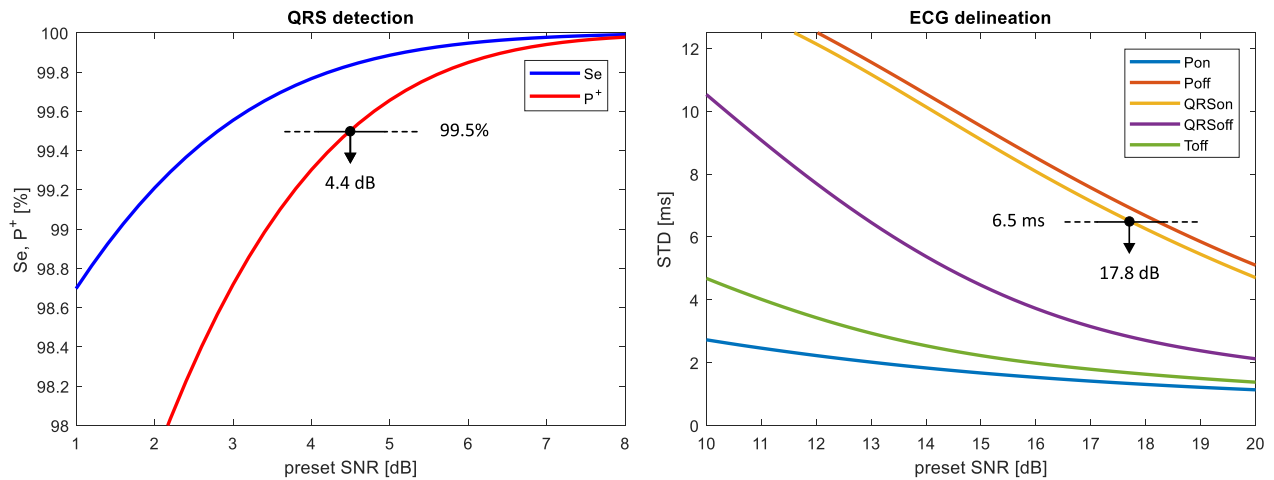


Fig. 8. Visualization of QRS complex detection (Realistic noise-free ECG signal with Real muscle artifact) and ECG delineation (Realistic noise-free ECG signal with Model muscle noise) algorithms results crossing the accuracy limits in detail.

TABLE III
ACCURACY OF QUALITY SEGMENTS DETECTION

	Without rules	With rules
Se [%]	94.29	91.06
P ⁺ [%]	37.56	88.39
m±s [ms]	-37±612	96±720
Number of segments (reference)	19.3	15.6
Number of segments (detected)	60.6	16.1

Number of segments – average number of segments per signal. Tolerance window for quality borders detection was set 1.5 sec.

TABLE IV
COINCIDENCE MATRIX OF SEGMENTS QUALITY CLASSIFICATION

%		Actual		
		Q1	Q2	Q3
Detected	Q1	32,88	0,51	0,00
	Q2	1,03	32,34	0,78
	Q3	0,05	0,89	31,52

%		Actual		
		Q1	Q2	Q3
Detected	Q1	32,86	0,33	0,24
	Q2	1,32	29,89	0,71
	Q3	0,65	0,95	33,05

which is more than three times higher than its reference value. This excessive signal quality segmentation is causing low P⁺.

In Table IV, the coincidence matrix of segments quality classification for both algorithm versions (with/without correction rules) is provided. The sum of diagonal values (green) describes the overall correct quality classification. In both cases, the signals have correctly classified quality in more than 95% of the time. The sum of values under the diagonal describes misclassification in cases when the actual quality is higher than the detected one. This type of error influences the type of

consequent analysis but the results are valid. The sum of values above the diagonal describes misclassification in cases when the actual quality is lower than the detected one. This type of error influences the type of consequent analysis with the significant misclassification error (with/without correction rules) around 1.3%.

In Fig. 9, an example of quality classification without (left) and with (right) correction rules is highlighted. The algorithm without correction rules fragments the signal quality excessively in the cases when the estimated SNR value oscillates around one of the thresholds which can be seen especially in the time between 600 and 800 s. The algorithm with correction rules prevents such excessive signal quality segmentation.

Based on the results, it was decided to further use the version of the algorithm with correction rules. Its overall sensitivity and positive predictivity of borders detection are around 90% with standard deviation under 1 s. The overall accuracy in term of quality classification including the misclassification with trusted analysis reaches 98.7% of the time.

B. Real Dataset

In this part, the reliability of the whole segmentation pipeline on real ECG signals is tested. However, it cannot be used the same accuracy criterion as for the artificial dataset (Se, P⁺ and coincidence matrix). The reason is that there is missing the reference information about quality segments distribution. As a criterion, it is used the ability of QRS detection and ECG delineation algorithms to reliably perform ECG analysis with respect to given segment quality. The reference QRS and other significant points positions were extracted from simultaneously measured standard 12-lead ECG. These points were obtained using QRS detection [42] and ECG delineation [43] algorithms and subsequently corrected by Holter ECG expert. The whole process of delineation and correction is very laborious and time consuming. Therefore, only three subjects were used for validation of designed algorithm.

One of the measurement of four ECG leads while performing predefined activities for 50 minutes is shown in Fig. 10. The type

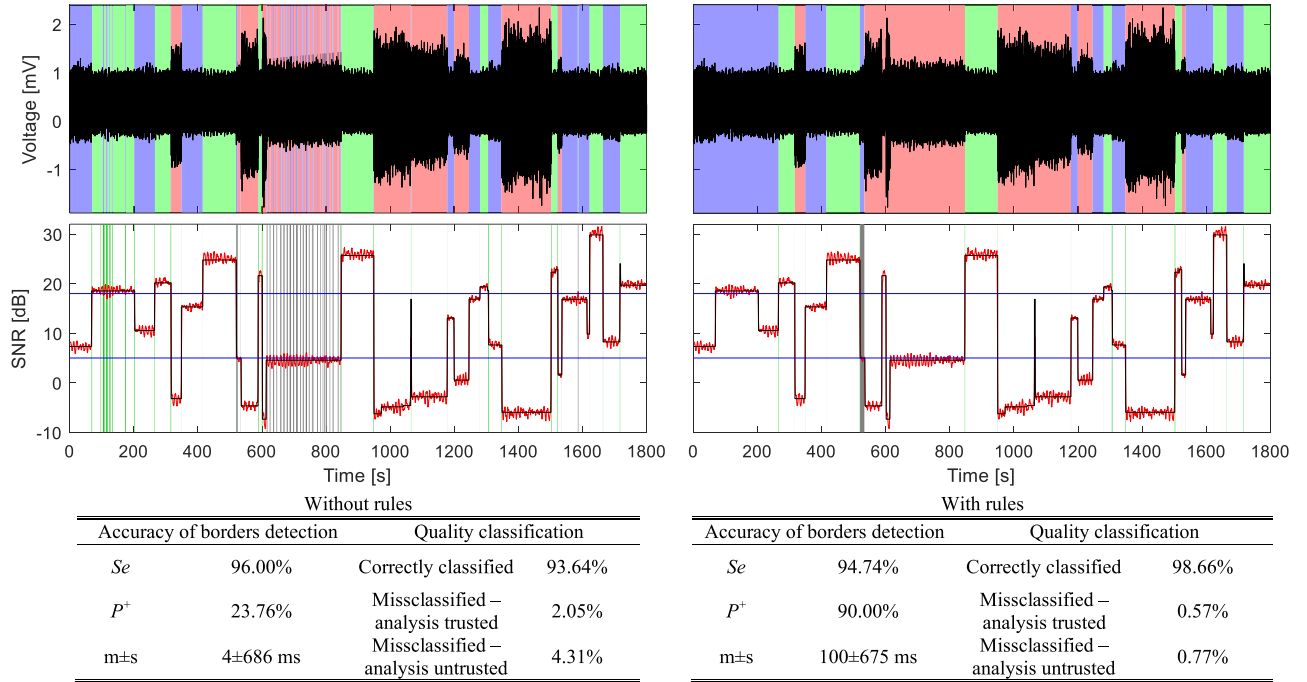


Fig. 9. Example of quality classification without (left) and with (right) correction rules. Top: green color highlights segments of Q1 quality, blue color highlights segments of Q2 quality and red color highlights segments of Q3 quality. Middle: Black color highlights setting of artificial ECG signal SNR levels. Red color highlights the estimated SNR levels. SNR thresholds are marked blue. Green and grey colors highlight misclassified quality with trusted and untrusted consequent analysis respectively. Bottom: The accuracy of segments borders detection and quality classification.

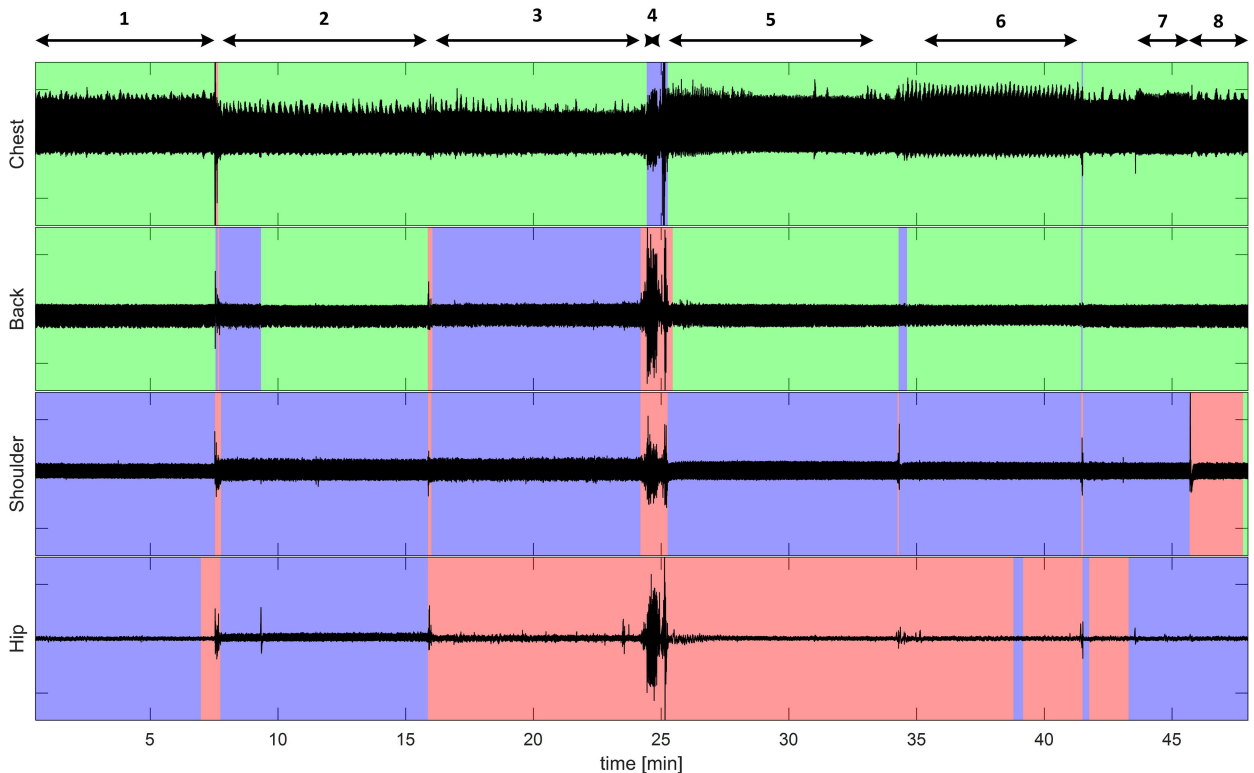


Fig. 10. Result of the real dataset segmentation. Green color marks the best quality class, blue color is used for the middle quality class and red color marks the worst quality segments. The dataset consists of four simultaneously measured leads (chest, back, shoulder and hip) during performing predefined activities which are indicated at the top part of the figure (1 – supine, 2 – sitting, 3 – standing, 4 – squats, 5 – supine, 6 – slow deep breathing, 7 – fast deep breathing, 8 - supine).

TABLE V
OVERALL RESULTS OF ECG ANALYSIS IN DIFFERENT QUALITY SEGMENTS

	Q1 (full wave analysis)	Q2 (QRS detection)	Q3 (no analysis)
Quality class information	236.05 min 46.75% of time 15260 beats	209.46 min 41.48% of time 13870 beats	59.44 min 11.77% of time 4467 beats
QRS detection	$Se = 99.99\%$ $P^+ = 99.99\%$	$Se = 99.73\%$ $P^+ = 99.76\%$	$Se = 85.27\%$ $P^+ = 90.65\%$
ECG delineation	$QRS_{on} = 4.54 \text{ ms}$ $QRS_{off} = 5.59 \text{ ms}$ $P_{on} = 14.91 \text{ ms}$ $P_{off} = 10.11 \text{ ms}$ $T_{off} = 6.83 \text{ ms}$	$QRS_{on} = 12.41 \text{ ms}$ $QRS_{off} = 13.92 \text{ ms}$ $P_{on} = 20.28 \text{ ms}$ $P_{off} = 21.83 \text{ ms}$ $T_{off} = 15.05 \text{ ms}$	$QRS_{on} = 15.87 \text{ ms}$ $QRS_{off} = 19.89 \text{ ms}$ $P_{on} = 24.59 \text{ ms}$ $P_{off} = 25.35 \text{ ms}$ $T_{off} = 23.44 \text{ ms}$

Red number indicates that the criterion for reliable QRS detection or reliable ECG delineation is not met.

and duration of each activity is indicated at the upper part of the figure. The measured subject performed a sequence of eight activities (supine, sitting, standing, squads, supine, slow and fast deep breathing, supine). Designed segmentation algorithm analyzed the signals quality. The resulting segments distribution is labelled by color boxes. Green marks the best quality class (allowing full wave analysis), blue is used for the middle quality class (only QRS detection is possible) and red marks the worst quality segments with noise levels preventing any type of reliable analysis. It is obvious, that ECG signals differ in quality among the leads and vary in time.

To verify the reliability of performed segmentation, the ECG signals were analyzed by both QRS detection [42] and ECG delineation [43] algorithms. The results are shown in Table V, where can be observed the overall results for each quality segment type through all three measured subjects. In worst quality segments (Q3), the Se and P^+ of QRS detection reach around 90% and ECG delineation failed in 4 out of 5 cases. In middle quality segments (Q2), the Se and P^+ of QRS detection accomplish criteria by crossing 99.5% and ECG delineation failed in 4 out of 5 cases. In best quality segments (Q1), the Se and P^+ of QRS detection reach almost 100% and ECG delineation accomplished the given criteria in 4 out of 5 cases.

It was chosen an interesting part of ECG signal measured from Back (all quality segment types are present) to demonstrate the achieved results in more detail. This part of ECG signal is plotted in Fig. 11. In the upper panel, there is the whole interesting part of the signal. The middle panel highlights the continuous SNR estimation (red) and segmentation thresholds (blue). The panels in lower part of the figure are zooms of times where signal quality changes. The results demonstrate Q3 quality segments (red) where both QRS complex detection and ECG delineation failed. The results of QRS detection or ECG delineation which don't meet the criterion are marked by red font. In Q2 quality segment (blue), ECG delineation failed but QRS complex detection is still reliable. In Q1 quality segments (green), QRS complex detection and also ECG delineation with exception of P wave is reliable. The problem with P wave detection (in this case) is caused by oscillating SNR values near the upper threshold.

The designed segmentation algorithm was verified on real dataset by consequent segments analysis using QRS detection and ECG delineation algorithms. The results demonstrate that

the proposed method is reliable with respect to consequent tailored analysis.

IV. DISCUSSION

ECG analysis is a well-accepted cardiovascular monitoring approach; however, its use has been limited to in-clinic and Holter patient monitoring. As consumer- and clinical-grade wearable technologies become more commonplace, the need for remote monitoring is also likely to increase. In fact, wearable technology continues to capture the interest of consumers and is riding an upward trend. The market saw a total of 105 million shipments during 2018 worth more than \$19 billion at retail value. This represents year-on-year increase of 10% in shipments and 17% in value [45]. Arguably, the value of wearable technologies is directly related to the quality and quantity of meaningful findings generated. Given the limited data storage capacity of wearable technologies and the increasing magnitude of the data the devices generate, real-time on-device or cloud data processing is necessary. In both cases, it is advantageous to characterize data quality, which may be impacted by improper attachment, sensor failure, or physiologic noise in order to reduce the data amount and the computational load and to permit tailored analysis or data transmission.

The issue of ECG signal quality estimation was the topic of the competition Computing in Cardiology Challenge 2011 (CINC) [46]. A total of 49 teams and individuals participated in this challenge. A wide variety of methods have been published to distinguish between acceptable and unacceptable data quality for further processing. The most successful algorithms used a wide range of features including entropy [47], higher order moments [48], QRS positions [49], [50], signal-to-noise ratio [51] and inter-lead information [48], [52]. The classification stage of the algorithms was realized e.g., by support vector machines [48], [53], decision trees [54] or heuristic rules [55]. In contrast to proposed study, all of these algorithms were developed for 12-lead 10 seconds ECG data. Moreover, the required classification was only to binary decide, whether the whole signal has acceptable or unacceptable quality. From these two reasons, the CINC Challenge data were not used. The proposed scheme is designed to identify which parts of long-term signals have sufficient quality for reliable analysis.

Nonetheless, algorithmic similarities and differences must be considered, particularly in the case of other approaches based on the signal-to-noise ratio. For example, Hayn *et al.* [51] used SNR as a one of three parameters for determining the signal quality. SNR is estimated as the amplitude of the lowest detected QRS complex, divided by the highest value of non-“QRS signal”. However, unlike the approach proposed in this paper, this method requires prior QRS detection, does not generate a continuous SNR curve, and does not take into account that the quality of a single record can change significantly over brief durations.

Another collection of algorithms was based on an estimation of noise-free signal curvature and subsequent calculation of the signal-to-noise ratio. Iravani and Tung [56] estimated the noise-free signal by averaging different ECG cycles, subtracting

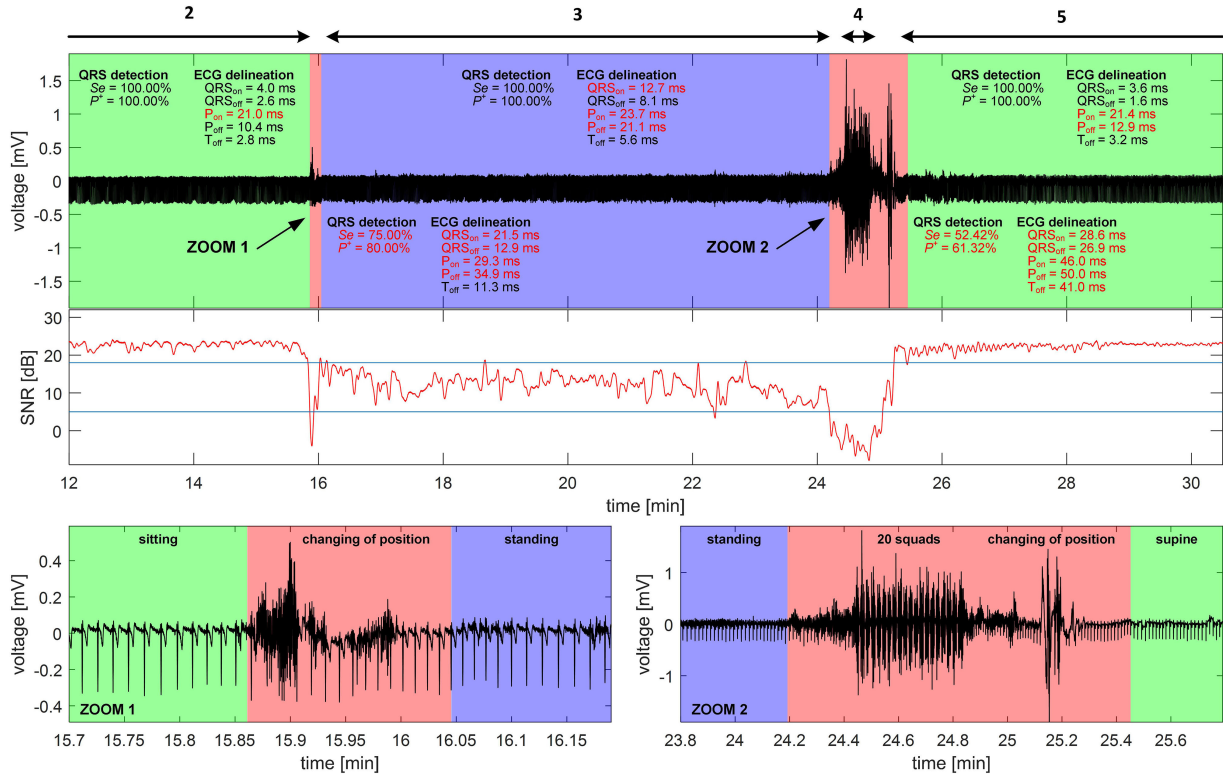


Fig. 11. Result of segmentation and analysis of an interesting part of ECG signal measured from Back (12 – 30.5 minutes, all quality segment types are present). Top panel: the whole interesting part of the signal with five segments and their analysis results. The results of QRS detection or ECG delineation which don't meet the criterion are marked by red font. Middle panel: the estimated SNR curve (red) and segmentation thresholds (blue). Low panels: zooms of times where signal quality changes. Green area marks the best quality segments, blue area marks the middle quality segments and red area marks the worst quality segments. The activities performing during the measurement are indicated in the upper part of the figure (2 – sitting, 3 – standing, 4 – squats, 5 – supine).

the average from the original signal, and then computing the SNR; accordingly, because this method requires a large window of samples to create the “noise-free signal,” it is less applicable for real-time wearable devices. Del Río *et al.* [57] proposed a method of extracting the ECG signal from the raw signal using least mean square (LMS) adaptive filtering to compute the noise content. This LMS approach requires a model of the desired signal as an input to the system. In contrast to these alternatives, the method proposed in this paper relies only on, and can adapt to, the characteristics of the input signal.

There are also some recent studies, which cover the topic of the ECG signal quality evaluation. Shahriari *et al.* [6], proposed a method of ECG quality assessment based on structural image similarity metric. Authors capture an image of multi-lead ECG plot with conventional time and amplitude scales, which is then subjected to a machine learning classification. This algorithm mimics how a human expert visually assesses the ECG signal quality. Shahriari’s method is not suitable for real-time applications and long-term signals. It also provides only binary decision and used quality parameters are not directly dependent on noise. Tobón *et al.* [8] proposed modulation spectral-based quality index which takes into account ECG spectral components. The method is based on the energy calculation in modulated spectrogram of short ECG segment. This method seems to have some quasi real-time and continuous quality estimation potential but

not in the presented form. The method resulted in a single quality index per whole ECG record and propose only binary decision whether the quality is acceptable or unacceptable. Morgado *et al.* [58] used an algorithm for 12-lead ECG quality evaluation based on cross-correlation among different leads. Morgado’s method proposes again only binary decision. Moreover, its principle is based on similarities between different leads and thus it is not suitable for single-lead application.

None of the above-mentioned algorithms meet all criteria important for long-term free-living ECG monitoring such as continuous quality assessment, real-time processing, single-lead processing, quality classes suitable for consequent tailored analysis, or quality parameters directly dependent on present noise. On the other hand, the algorithm proposed in this paper is designed to process both single-lead records and multi-lead records (lead by lead independently) in a real time using only short-time buffer. The algorithm assesses the signal quality continuously by computing SNR (which directly depends on noise level) in sliding window and consequent application of thresholding and decision rules. The final product is a detailed signal quality annotation enabling tailored signal quality-specific analysis.

The proposed processing pipeline was set and tested on the artificial data set which was created by combining different noise-free signals and different noises. The first result is an identification of the range of reliable SNR estimation. This

range is from -20 to 30 dB for both tested methods (Time and Time-frequency domain approach). The proposed time domain approach was demonstrated to provide higher accuracy than the frequency domain approach within this range and thus it is recommended for further use. The second result is determining the SNR thresholds setting to distinguish different quality classes. Specifically, three logical classes were determined (Q1 – full wave analysis possible, Q2 – QRS detection possible, Q3 – no analysis possible). Using the algorithm for automatic QRS detection and ECG delineation, the SNR thresholds of 5 and 18 dB were found. The thresholds permit distinguishing between quality classes and satisfy conditions for reliable consequent analysis. The SNR thresholds for the quality differentiation were set based on analysis of a large amount of data. If a user wants to have the subsequent analysis even more reliable, the thresholds may be moved arbitrarily larger to their desired effect. On the other hand, the amount of extractable diagnostic information for tailored analysis artificially decreases. The ECG curve shape is different among leads, which means that it may be more or less difficult to reliably delineate the ECG signal in different leads. The influence of lead selection on the reliability of delineation is beyond the scope of this study. The delineation error can be also caused by connecting of subsequent segments (with lower quality) within the segmentation rules. The next results are Sensitivity (91.06%) and Positive predictivity (88.39%) of quality segments borders detection and correct quality classification in time percentage (95.80%). From the classification error (4.20% of the time), 2.92% is the misclassification which do not influence the consequent analysis. Only 1.28% of time can produce the untrusted analysis. The contrast between Se , P^+ (around 90%) and time percentage quality classification (around 96%) is due to the fact that e.g., quality segments with the real duration slightly above 3 or 15 seconds (correction rules) is estimated slightly less than 3 or 15 seconds (due to the slower increasing and descending edge of the estimated SNR curve) and thus eliminated according to the rules. This have greater impact on Se and P^+ (which reflects only the number of segments boundaries found), but it has only small effect on time percentage quality classification because it is exclusively connected with a short (3 and 15 seconds) segments.

The accuracy and reliability of the algorithm was also validated on the real dataset. The dataset was obtained by measuring four single-lead ECGs and one 12-leads standard ECG on three subjects during different predefined activities. The 12-leads standard ECG was used as a reference for precise extraction of ECG significant points, while the single-lead ECGs were used for testing the ability of QRS detection and ECG delineation algorithm to correctly detect these points. The assumptions were: 1) In the lowest quality segments none of the significant points should be reliably detected, 2) In the middle quality segments only the QRS complexes should be detectable accurately, and 3) In the highest quality segments all of the significant points should be detectable accurately. The first two assumptions were completely satisfied and the third assumption was not satisfied for the P wave onset. However, the P wave onset case is not specific to proposed methodology and set parameters but rather a limitation of the detection and delineation algorithms.

The P wave detection and delineation algorithms are comparable with other published methods. However, unfortunately, the reliable detection of the P wave and its boundaries remains an open area of investigation. The results of algorithms tested on physiological data can reach satisfying results, e.g., [59], [60]. The results of algorithms tested on pathological data are significantly worse [61], [62]. The reliability of the proposed method (the accuracy of the threshold setting) is dependent on the reliability of these algorithms, and with the improvement of these algorithms in the future, it is possible to further refine the threshold values that distinguish between the different quality classes. The threshold values were heuristically selected on a large set of data (real and artificial). The proposed methodology is generally valid and can be used to select the threshold values under different condition e.g., different noise-free estimator, different delineation algorithms or even with a higher number of quality classes.

V. CONCLUSION

There are many clinical and non-clinical health reasons to monitor ECG signals. To do so on a wearable platform is challenging due to the limited available computational, memory, and battery resources. Moreover, the quality of the data may vary depending on the device, device placement, and person activity. In order to appropriately process the ECG signal and report meaningful findings it is important to characterize the quality of the signal prior to analysis. The proposed novel approach based on continuous SNR estimation and decision rules to obtain detail quality annotation can facilitate real-time embedded analysis of ECG signals directly on device. It was demonstrated that continuous monitoring of the ECG quality and classification of the quality into more than two classes may improve the possibilities of follow-up analysis and diagnosis of electrocardiograms. In this work, the new approach has been set and tested on artificial data and validated in a unique real volunteer study. The future objective is to expand this work by fusion of ECG data with other sensors data (e.g., accelerometer data) to increase the robustness and accuracy of the ECG quality estimation in free-living condition. The algorithm targets primarily real-time applications and the monitoring the important cardiovascular parameters of people with increased physical and environmental load but is general to all physiologic conditions.

ACKNOWLEDGMENT

The authors wish to thank LCDR Joshua Swift from ONR Code 342 and Dr. Stephen O'Regan from ONR Global Central and Eastern European Office for their support. The authors would also like to acknowledge the effort of Daniel Schwab and his colleagues in the Special Purpose Processor Development Group, Mayo Clinic for their effort in preparing the devices and facilitating the data management and the staff of the Biomedical Imaging Resource, Mayo Clinic for their feedback and infrastructure support.

REFERENCES

- [1] World Health Organization, "Cardiovascular diseases," May 2017. [Online]. Available: <http://www.who.int/mediacentre/factsheets/fs317/en/>
- [2] T. A. Gaziano, "Cardiovascular disease in the developing world and its cost-effective management," *Circulation*, vol. 112, no. 23, pp. 3547–3553, 2005.
- [3] B. J. Gersh *et al.*, "The epidemic of cardiovascular disease in the developing world: Global implications," *Eur. Heart J.*, vol. 31, no. 6, pp. 642–648, 2010.
- [4] D. S. Celermajer *et al.*, "Cardiovascular disease in the developing world," *J. Am. Coll. Cardiol.*, vol. 60, no. 14, pp. 1207–1216, 2012.
- [5] L. Sörnmo and P. Laguna, *Bioelectrical Signal Processing in Cardiac and Neurological Applications*, Cambridge, Massachusetts, United States: Elsevier Academic Press, 2005.
- [6] Y. Shahriari *et al.*, "Electrocardiogram signal quality assessment based on structural image similarity metric," *IEEE Trans. Biomed. Eng.*, vol. 65, no. 4, pp. 745–753, Apr. 2018.
- [7] Y. Bai *et al.*, "Is the sequence of superalarm triggers more predictive than sequence of the currently utilized patient monitor alarms?," *IEEE Trans. Biomed. Eng.*, vol. 64, no. 5, pp. 1023–1032, May 2017.
- [8] D. P. Tobón *et al.*, "MS-QI: A modulation spectrum-based ECG quality index for telehealth applications," *IEEE Trans. Biomed. Eng.*, vol. 63, no. 8, pp. 1613–1622, Aug. 2016.
- [9] U. Satija, B. Ramkumar, and M. S. Manikandan, "A review of signal processing techniques for electrocardiogram signal quality assessment," *IEEE Rev. Biomed. Eng.*, vol. 11, pp. 36–52, Feb. 28, 2018.
- [10] A. Némcová *et al.*, "A comparative analysis of methods for evaluation of ECG signal quality after compression," *Biomed Res. Int.*, vol. 2018, 2018, Art. no. 1868519.
- [11] C. L. Tsien and J. C. Fackler, "Poor prognosis for existing monitors in the intensive care unit," *Crit. Care Med.*, vol. 25, no. 4, pp. 614–619, 1997.
- [12] I. Zepeda-Carapia *et al.*, "Measurement of skin-electrode impedance for a 12-lead electrocardiogram," in *Proc. 2nd Int. Conf. Electr. Electron Eng.*, Mexico City, Mexico, 2005, pp. 193–195.
- [13] J. A. Sukor *et al.*, "Signal quality measures for pulse oximetry through waveform morphology analysis," *Physiol. Meas.*, vol. 32, no. 3, pp. 369–384, 2011.
- [14] Q. Li *et al.*, "Artificial arterial blood pressure artifact models and an evaluation of a robust blood pressure and heart rate estimator," *Biomed. Eng. Online*, vol. 8, 2009, Art. no. 13.
- [15] A. Alesanco and J. García, "Automatic real-time ECG coding methodology guaranteeing signal interpretation quality," *IEEE Trans. Biomed. Eng.*, vol. 55, no. 11, pp. 2519–2527, Nov. 2008.
- [16] C. Orphanidou *et al.*, "Signal-quality indices for the electrocardiogram and photoplethysmogram: Derivation and applications to wireless monitoring," *IEEE J. Biomed. Health Inform.*, vol. 19, no. 3, pp. 832–838, May 2015.
- [17] J. Wang, "A new method for evaluating ECG signal quality for multi-lead arrhythmia analysis," in *Proc. Comput. Cardiol.*, Memphis, TN, USA, 2002, pp. 85–88.
- [18] Q. Li *et al.*, "Robust heart rate estimation from multiple asynchronous noisy sources using signal quality indices and a Kalman filter," *Physiol. Meas.*, vol. 29, no. 1, pp. 15–32, 2008.
- [19] A. Bartolo *et al.*, "An arrhythmia detector and heart rate estimator for overnight polysomnography studies," *IEEE Trans. Biomed. Eng.*, vol. 48, no. 5, pp. 513–521, May 2001.
- [20] J. Allen and A. Murray, "Assessing ECG signal quality on a coronary care unit," *Physiol. Meas.*, vol. 17, no. 4, pp. 249–258, 1996.
- [21] N. V. Thakor, "From holter monitors to automatic defibrillators: Developments in ambulatory arrhythmia monitoring," *IEEE Trans. Biomed. Eng.*, vol. 31, no. 12, pp. 770–778, Dec. 1984.
- [22] Y. Kim and I.-Y. Cho, "Wearable ECG monitor: Evaluation and experimental analysis," in *Proc. Int. Conf. Inf. Sci. Appl.*, Jeju Island, South Korea, pp. 1–5, 2011.
- [23] L. Smital *et al.*, "Adaptive wavelet wiener filtering of ECG signals," *IEEE Trans. Biomed. Eng.*, vol. 60, no. 2, pp. 437–445, Feb. 2013.
- [24] D. J. Schwab *et al.*, "A measurement-quality body-worn physiological monitor for use in harsh environments," *Am. J. Biomed. Eng.*, vol. 4, no. 4, pp. 88–100, 2014.
- [25] J. L. Willems *et al.*, "Establishment of a reference library for evaluating computer ECG measurement programs," *Comput. Biomed. Res.*, vol. 18, no. 5, pp. 439–457, 1985.
- [26] R. Smíšek *et al.*, "CSE database: Extended annotations and new recommendations for ECG software testing," *Med. Biol. Eng. Comput.*, vol. 55, no. 8, pp. 1473–1482, 2017.
- [27] A. L. Goldberger *et al.*, "Physiobank, physiotoolkit, and physionet," *Circulation*, vol. 101, no. 23, pp. e215–e220, 2000.
- [28] P. E. McSharry *et al.*, "A dynamical model for generating synthetic ECG signals," *IEEE Trans. Biomed. Eng.*, vol. 50, no. 3, pp. 289–294, Mar. 2003.
- [29] G. B. Moody *et al.*, "A noise stress test for arrhythmia detectors," in *Proc. Comput. Cardiol.*, Park City, UT, USA, 1984, pp. 381–384.
- [30] D. Farina and R. Merletti, "Comparison of algorithms for estimation of EMG variables during voluntary isometric contractions," *J. Electromyogr. Kinesiol.*, vol. 10, no. 5, pp. 337–349, 2000.
- [31] E. Shwedky *et al.*, "A nonstationary model for the electromyogram," *IEEE Trans. Biomed. Eng.*, vol. BME-24, no. 5, pp. 417–424, Sep. 1977.
- [32] D. Farina and R. Merletti, "A novel approach for precise simulation of the EMG signal detected by surface electrodes," *IEEE Trans. Biomed. Eng.*, vol. 48, no. 6, pp. 637–646, Jun. 2001.
- [33] B. K. Gilbert *et al.*, "A measurement-quality body-worn sensor-agnostic physiological monitor for biomedical applications," *Am. J. Biomed. Eng.*, vol. 5, no. 2, pp. 34–66, 2015.
- [34] W. J. Hurd *et al.*, "Tri-axial accelerometer analysis techniques for evaluating functional use of the extremities," *J. Electromyogr. Kinesiol.*, vol. 23, no. 4, pp. 924–929, 2013.
- [35] V. Lugade *et al.*, "Validity of using tri-axial accelerometers to measure human movement—Part I: Posture and movement detection," *Med. Eng. Phys.*, vol. 36, no. 2, pp. 169–176, 2014.
- [36] P. Kligfield *et al.*, "Recommendations for the standardization and interpretation of the electrocardiogram: part I: The electrocardiogram and its technology a scientific statement from the American Heart Association Electrocardiography and Arrhythmias Committee, Council on Clinical Cardiology; the American College of Cardiology Foundation; and the Heart Rhythm Society endorsed by the International Society for Computerized Electrocardiology," *J. Am. Coll. Cardiol.*, vol. 49, no. 10, pp. 1109–1127, 2007.
- [37] P. Lander and E. J. Berbari, "Time-frequency plane Wiener filtering of the high-resolution ECG: Background and time-frequency representations," *IEEE Trans. Biomed. Eng.*, vol. 44, no. 4, pp. 247–255, Apr. 1997.
- [38] H. Kestler *et al.*, "De-noising of high-resolution ECG signals by combining the discrete wavelet transform with the Wiener filter," in *Proc. Comput. Cardiol.*, Cleveland, OH, USA, 1998, pp. 233–236.
- [39] B.-U. Köhler, C. Hennig, and R. Orglmeister, "The principles of software QRS detection," *IEEE Eng. Med. Biol. Mag.*, vol. 21, no. 1, pp. 42–57, Jan.–Feb. 2002.
- [40] Z. Zidelmal *et al.*, "QRS detection using S-Transform and Shannon energy," *Comput. Meth. Programs Biomed.*, vol. 116, no. 1, pp. 1–9, 2014.
- [41] J. Willems, "Recommendations for measurement standards in quantitative electrocardiography," *Eur. Heart J.*, vol. 6, no. 10, pp. 815–825, 1985.
- [42] M. Vitek, J. Hruběš, and J. Kozumplík, "A wavelet-based QRS delineation in multilead ECG signals: Evaluation on the CSE database," in *Proc. 19th Bienn. Int. EURASIP Conf. BIOSIGNAL*, Brno, Czech Republic, 2008, pp. 177–180.
- [43] M. Vitek *et al.*, "A wavelet-based ECG delineation in multilead ECG signals: Evaluation on the CSE database," in *Proc. World Congr. Med. Phys. Biomed. Eng.*, Munich, Germany, 2009, pp. 177–180.
- [44] M. Vitek *et al.*, "A wavelet-based ECG delineation with improved P wave offset detection accuracy," in *Proc. 20th Bienn. Int. EURASIP Conf. BIOSIGNAL*, Brno, Czech Republic, 2010, pp. 160–165.
- [45] FutureSource Consulting, "Wearables riding high, 100m+ units shipped in 2018," Jul. 2019. [Online]. Available: <https://futuresource-consulting.com/press-release/consumer-electronics-press/wearables-riding-high-100mplus-units-shipped-in-2018/>
- [46] I. Silva *et al.*, "Improving the quality of ECGs collected using mobile phones: The physionet/computing in cardiology challenge 2011," in *Proc. Comput. Cardiol.*, Hangzhou, China, 2011, pp. 273–276.
- [47] H. Xia *et al.*, "Computer algorithms for evaluating the quality of ECGs in real time," in *Proc. Comput. Cardiol.*, Hangzhou, China, 2011, pp. 369–372.
- [48] G. D. Clifford *et al.*, "Signal quality indices and data fusion for determining acceptability of electrocardiograms collected in noisy ambulatory environments," in *Proc. Comput. Cardiol.*, Hangzhou, China, 2011, pp. 285–288.
- [49] T. H. C. Tat *et al.*, "Physionet challenge 2011: Improving the quality of electrocardiography data collected using real time QRS-complex and T-wave detection," in *Proc. Comput. Cardiol.*, Hangzhou, China, 2011, pp. 441–444.

- [50] L. Johannessen, "Assessment of ECG quality on an Android platform," in *Proc. Comput. Cardiol.*, Hangzhou, China, 2011, pp. 433–436.
- [51] D. Hayn *et al.*, "ECG quality assessment for patient empowerment in mHealth applications," in *Proc. Comput. Cardiol.*, Hangzhou, China, 2011, pp. 353–356.
- [52] N. Kalkstein *et al.*, "Using machine learning to detect problems in ECG data collection," in *Proc. Comput. Cardiol.*, Hangzhou, China, 2011, pp. 437–440.
- [53] J. Kužílek *et al.*, "Data driven approach to ECG signal quality assessment using multistep SVM classification," in *Proc. Comput. Cardiol.*, Hangzhou, China, 2011, pp. 453–455.
- [54] S. Zaunseder *et al.*, "CinC challenge—Assessing the usability of ECG by ensemble decision trees," in *Proc. Comput. Cardiol.*, Hangzhou, China, 2011, pp. 277–280.
- [55] B. E. Moody, "Rule-based methods for ECG quality control," in *Proc. Comput. Cardiol.*, Hangzhou, China, 2011, pp. 361–363.
- [56] S. Iravanian and L. Tung, "A novel algorithm for cardiac biosignal filtering based on filtered residue method," *IEEE Trans. Biomed. Eng.*, vol. 49, no. 11, pp. 1310–1317, Nov. 2002.
- [57] B. Del Río *et al.*, "Assessment of different methods to estimate electrocardiogram signal quality," in *Proc. Comput. Cardiol.*, Hangzhou, China, 2011, pp. 609–612.
- [58] E. Morgado *et al.*, "Quality estimation of the electrocardiogram using cross-correlation among leads," *Biomed. Eng. Online*, vol. 14, 2015, Art. no. 59.
- [59] A. Ghaffari *et al.*, "A robust wavelet-based multi-lead electrocardiogram delineation algorithm," *Med. Eng. Phys.*, vol. 31, no. 10, pp. 1219–1227, 2009.
- [60] J. P. Martínez *et al.*, "A wavelet-based ECG delineator: Evaluation on standard databases," *IEEE Trans. Biomed. Eng.*, vol. 51, no. 4, pp. 570–581, Apr. 2004.
- [61] F. Portet, "P wave detector with PP rhythm tracking: Evaluation in different arrhythmia contexts," *Physiol. Meas.*, vol. 29, no. 1, pp. 141–155, 2008.
- [62] P. Laguna, R. Jané, and P. Caminal, "Automatic detection of wave boundaries in multilead ECG signals: Validation with the CSE database," *Comput. Biomed. Res.*, vol. 27, no. 1, pp. 45–60, 1994.